

The fate of graphite in prograde metamorphism of pelites: An example from the Ballachulish aureole, Scotland

David R.M. Pattison*

Department of Geology and Geophysics, University of Calgary, Calgary, Alberta, Canada, T2N 1N4

Received 16 February 2005; accepted 16 August 2005

Available online 29 November 2005

Abstract

Graphite-bearing slates and phyllites (0.4–1.2 vol.% graphite) are progressively metamorphosed in the 3 kbar aureole of the 425 Ma Ballachulish intrusion, Scotland. Two major dehydration reactions are crossed: the chlorite-out reaction at ca. 550 °C (forming cordierite + biotite), and the muscovite-out reaction at 625 °C (forming Al₂SiO₅ + K-feldspar). Graphite persists to the highest grades and shows no significant variation in abundance with grade, except for a possible decrease in the highest grade rocks. Variable graphite abundance in rocks at the same grade reflects primary sedimentological heterogeneity. Texturally, graphite grains and aggregates in the rock matrix become coarser grained and more widely separated as grade increases. These thermally induced textural modifications of graphite are superimposed on mechanically induced features, such as graphite segregations along cleavages and crenulations, that formed prior to contact metamorphism. Mass balance modelling, assuming internal fluid generation, shows that the amount of graphite consumed during contact metamorphism in the aureole ranges between 0.1 and 0.3 vol.%, depending on the amount of chlorite and muscovite in the protolith. Because the amount of C dissolved in a C–O–H fluid decreases with increasing pressure, and the Ballachulish aureole is at relatively low pressure, these results are a maximum for regional metamorphism, suggesting that graphite will persist through a regional metamorphic cycle if it is initially present in volumes >ca. 0.2 vol.%.

© 2005 Published by Elsevier B.V.

Keywords: Graphite; Metapelites; Prograde metamorphism; Ballachulish aureole

1. Introduction

Graphite is a common accessory phase in metapelites (metamorphosed mudrocks, siltstones and wackes), typically occurring in the range 0.1–1.0 vol.% of the rock, but sometimes exceeding 25 vol.% (Grew, 1974; Morikiyo, 1986). The graphite is usually interpreted to represent metamorphosed carbonaceous material that accumulated in the original sediment. Several studies

have investigated the structural transformation of disordered carbonaceous material (loosely, bitumen) in unmetamorphosed shales and mudrocks to crystalline graphite in metamorphic rocks (e.g., French, 1964; Landis, 1971; Grew, 1974; Itaya, 1981; Buseck and Huang, 1985; Okuyama-Kusunose and Itaya, 1987; Wang, 1989; Wopenka and Pasteris, 1993; Beyssac et al., 2002).

The purpose of this paper is to assess what happens modally and texturally to graphite in prograde metamorphism of metapelitic rocks. Graphite dissolves into a hydrous fluid according to the reaction:



* Tel.: +1 403 220 3263; fax: +1 403 284 0074.

E-mail address: pattison@ucalgary.ca.

URL: <http://www.geo.ucalgary.ca/~pattison/>.

During prograde metamorphism, reaction of hydrous phyllosilicates such as chlorite and muscovite to produce less hydrous product phases such as cordierite results in the generation of a hydrous fluid phase that escapes the rock, e.g.:



(abbreviations of Kretz, 1983). Generation of hydrous fluid by reaction (2), combined with dissolution of graphite into this fluid by reaction (1) and escape of the fluid from the rock, means that graphite is expected to decrease in abundance as metamorphic grade increases. An unanswered question is by how much. Some indication that graphite is not consumed markedly as grade increases comes from the relatively widespread occurrence of graphitic granulite-facies pelitic gneisses thought to represent highly metamorphosed black shales (e.g., Cesare et al., 2003a and references therein), and diamond-bearing pelitic gneisses (e.g., Sobolev and Shatsky, 1990).

An accompanying question relates to the distribution and texture of graphite as grade increases. Graphite has been implicated in zones of anomalously high electrical conductivity in the middle and lower crust (Frost et al., 1989; Shankland et al., 1997; Crespo et al., 2004). These authors argued that continuous networks of angstrom-thickness graphite films along grain boundaries, produced during cooling of C–O–H fluids in high grade rocks, created the connectivity needed to achieve the observed electrical conductivity. Other studies have focused on coarser scale textural features that could achieve the same bulk conductivity. For example, Jödicke et al. (2004) showed that for similar absolute abundances of graphite, metapelitic rocks in which graphite grains had been mechanically segregated into discrete continuous seams had several orders of magnitude higher electrical conductivity than metapelitic rocks of the same carbon content in which graphite flakes were dispersed. The presence of a few such seams in a body of otherwise low conductivity rock could produce a bulk conductivity comparable to pervasive thin graphite films throughout the body of rock. Thus the texture and distribution of graphite may be as important to electrical conductivity as its absolute abundance.

The locality chosen for this study is the well-constrained metamorphic aureole surrounding the Ballachulish Igneous Complex, Scotland (Pattison and Harte, 1997), in which a graphitic metapelite unit can be followed up grade to the contact. Graphite abundance as a function of grade is compared with predictions

from thermodynamic modeling. Textural modification of graphite as grade increases is assessed using a combination of optical microscopy and carbon X-ray mapping on the electron microprobe. The results are then extrapolated to regional metamorphism, allowing some broader conclusions to be made regarding the fate and significance of graphite in the metamorphism of pelites.

2. The Ballachulish Igneous Complex and aureole

The Ballachulish Igneous Complex and aureole (Fig. 1a) is one of the world's most intensively studied plutonic–metamorphic complexes (Voll et al., 1991; Pattison and Harte, 1997). The 425 ± 4 Ma igneous complex (Fraser et al., 2004) was emplaced at a pressure of ca. 3 kbar (Pattison, 1989), equivalent to a depth of ca. 10 km, in metasediments belonging to the Dalradian Supergroup (Pattison and Voll, 1991). Prior to emplacement of the igneous complex, the host metasediments were regionally deformed and metamorphosed to Barrovian garnet-zone conditions (450–500 °C, 6 kbar; Pattison and Voll, 1991).

The intrusion consists of an outer orthopyroxene-bearing diorite shell (emplacement temperature ca. 1100 °C) surrounding a central body of granite (emplacement temperature ca. 850 °C), the latter emplaced when the central portion of the diorite was still partially molten (Weiss and Troll, 1989, 1991). A well developed contact aureole surrounds the intrusive complex. Isograds in pelitic rocks, the most abundant rock type in the aureole, can be mapped around the intrusion and range from development of cordierite 'spots' (ca. 550 °C) up to anatectic migmatization (700–800 °C) (Pattison and Harte, 1991). Based on the outermost occurrence of cordierite, the aureole ranges in width from 400–1700 m.

The contact metamorphism was mainly caused by intrusion of the diorite phase, with the later granite having little effect (Buntebarth, 1991). The duration of the contact metamorphic event, for temperatures above conditions of the cordierite-in reaction (ca. 550 °C), was about 500 Ka, whereas rocks in the inner aureole were hot enough to be partially molten (temperatures above ca. 660 °C) for about 270 Ka (Buntebarth, 1991). With the exception of some fluid-fluxed partial melting on the west flank of the complex, fluid communication between the intrusion and aureole was generally limited (Harte et al., 1991b; Ferry, 1996). There is no evidence for the development of a large-scale hydrothermal circulation system around the intrusion.

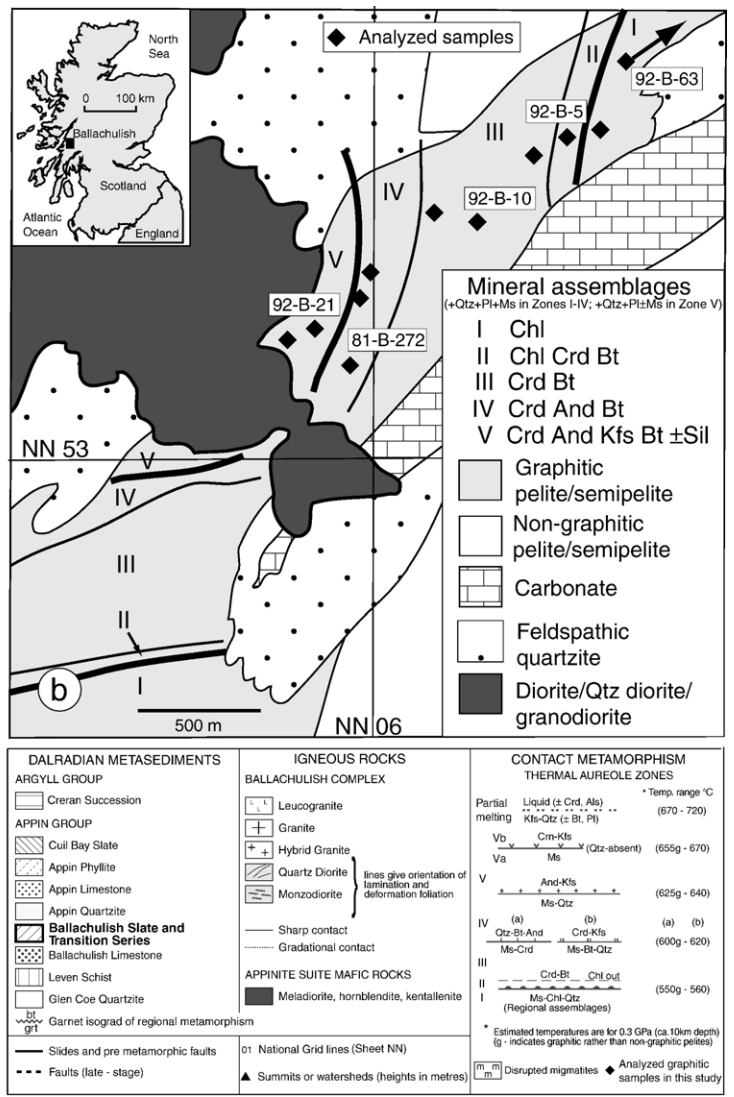
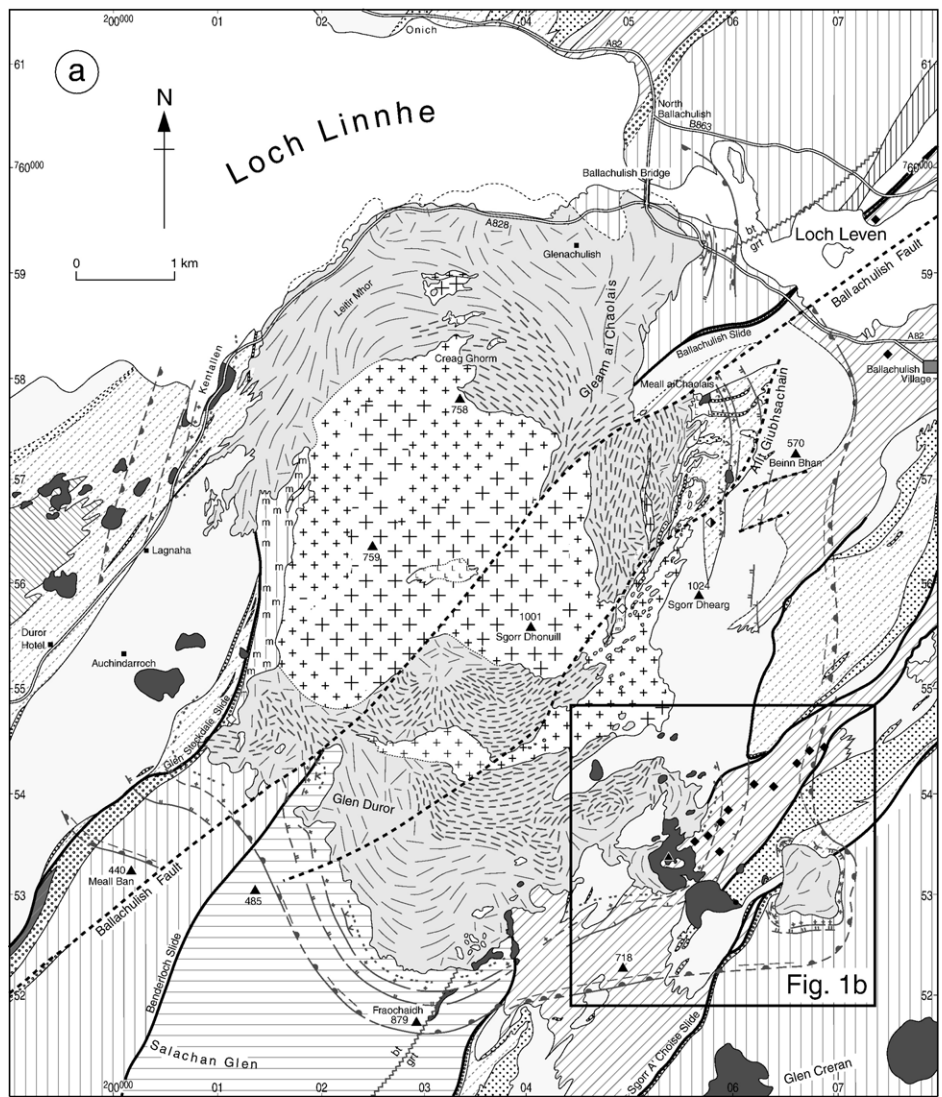


Fig. 1. (a) Geology of the Ballachulish area (modified from Fig. 7 of Pattison and Harte, 2001). (b) Location of analyzed samples.

D.R.M. Pattison / Lithos 88 (2006) 85–99

3. Petrology of the graphitic metapelites

Graphitic metapelites belonging to the Ballachulish Slate and Transition Series stratigraphic units (Pattison and Voll, 1991) occur at various places in the contact aureole (Fig. 1a). The focus of this study is a band of graphitic metapelite that can be traced continuously upgrade along strike in the southeast part of the aureole (Fig. 1b). Although the pre-intrusion regional metamorphic grade is in the garnet zone, the graphitic slates and phyllites themselves do not contain either garnet or biotite due to their relatively magnesian composition (Pattison and Harte, 1997, 2001).

Five mineral assemblage zones related to contact metamorphism, separated by isograds, have been mapped in the graphitic metapelite in Fig. 1b (Pattison and Harte, 1985, 1991). Fifty-eight samples spanning the range of grade were examined optically. Thirteen representative, relatively homogeneous, pelitic samples were chosen for whole rock carbon analysis (Fig. 2). A ca. $3 \times 3 \times 3$ cm³ cube of each sample was analyzed. Five of these samples were chosen for carbon X-ray mapping. Figs 3 and 4 show hand sample photographs and optical photomicrographs of rocks from the different metamorphic zones.

3.1. Whole rock analysis

Whole rock C was analyzed at Geochemical Laboratories, McGill University, using an induction furnace for combustion and an infrared detector for CO₂, and standard reference materials of a similar composition and C content as the samples. The output was then converted to weight percent C.

Variation in whole rock C content is shown in Fig. 2. C content varies from 0.35 to 1.02 wt.%. This corresponds to 0.4–1.2 vol.% graphite, using a 1.22 conversion factor of wt.% C to vol.% graphite, and assuming that all of the carbon in these carbonate-free rocks resides in graphite.

The data show considerable scatter, most likely reflecting primary sedimentological variations in carbon content in the original mud-rich sediments. C content shows no correlation with other whole rock parameters such as weight percent SiO₂ or Mg/(Mg+Fe). There is no evidence of a trend of increasing or decreasing carbon abundance with metamorphic grade between Zones I and IV, although there is an apparent drop in carbon abundance between Zones IV and V (more discussion below).

3.2. Analysis of graphite distribution and texture using carbon mapping

The distribution and texture of graphite in five representative samples was assessed by a combination of optical methods and carbon X-ray mapping (Figs. 4 and 5). The carbon X-ray images were collected from 500×500 μm areas using a JEOL JXA-8200 electron microprobe at the University of Calgary. Operating conditions were 15 kV potential, 30 nA current, focused beam, 100 ms dwell time, 0.5 μm step size and 1000×1000 steps. Carbon was detected on a JEOL synthetic layered diffraction element (LDE2) crystal. An ordinary commercially polished thin section was used, carbon-coated for routine microprobe analysis. Superior X-ray images would be obtained using more finely polished sections and silver as a conductive coat (E. Mathez, written communication, 2005). Despite

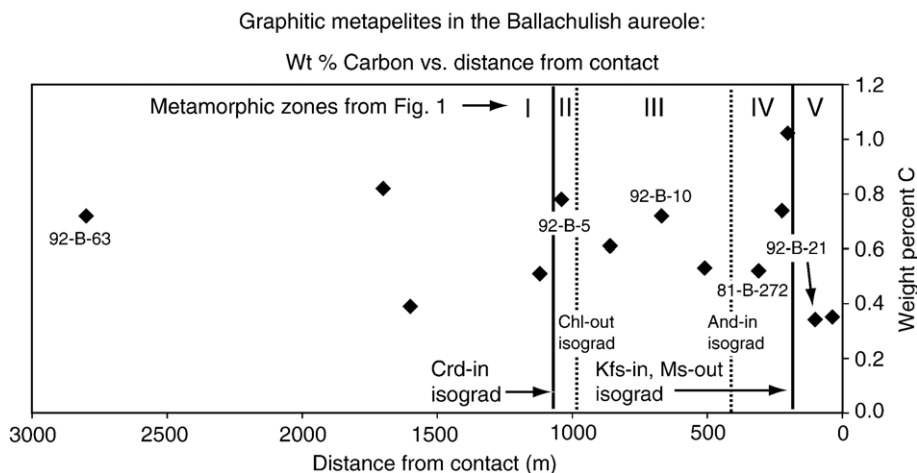


Fig. 2. Variation of whole rock carbon content with grade. Numbered samples are located in Fig. 1b.

Graphitic metapelites in the Ballachulish aureole

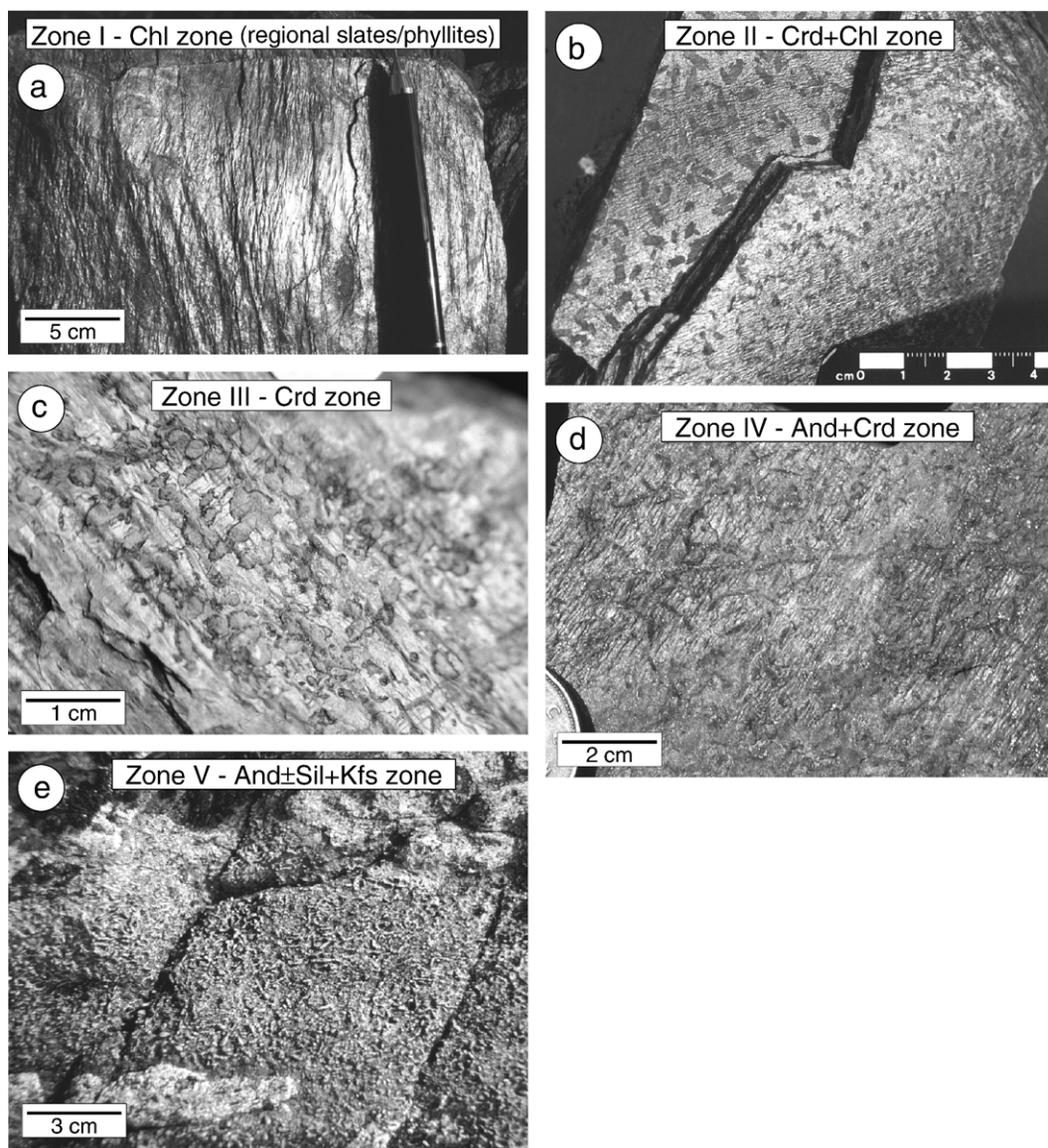


Fig. 3. Photographs of outcrop surfaces or hand samples from the five zones of contact metamorphism in the Ballachulish aureole. (a) Zone I—crenulated graphitic phyllite outside the aureole. (b) Zone II—cordierite porphyroblasts visible on schistosity surfaces. (c) Zone III—cordierite porphyroblasts with dark rims (due to pinitization of cordierite margins) in partially hornfelsed, crenulated phyllite. (d) Zone IV—elongate andalusite crystals visible on crenulated schistosity surfaces. (e) Zone V—densely recrystallized andalusite+K-feldspar hornfels.

these limitations, the X-ray signal from domains of concentrated carbon in the rock, such as graphite, can be clearly discerned as bright spots (see Fig. 5).

The main limitation to the technique relates to the scale of feature that can be detected. The pixel size in the images in this study, $0.5 \mu\text{m} \times 0.5 \mu\text{m}$, is about 10 times smaller than the diameter of the excitation volume for X-ray analysis for the listed operating conditions (ca. $5 \mu\text{m}$). Thus, even for sub-micron graphite

grains, the result may be a ‘blurred’ carbon signal that covers several pixels. For this reason, quantitative analysis of the X-ray images is not emphasized. Angstrom-scale features, such as along fractures and within silicate cleavages (e.g., Frost et al., 1989; Shankland et al., 1997; Mogk and Mathez, 2000; Ferraris et al., 2004), may not be detected at all.

Despite these limitations, comparison of Figs. 4 and 5 shows that the two methods give complementary results.

Photomicrographs of graphitic metapelites in the Ballachulish aureole

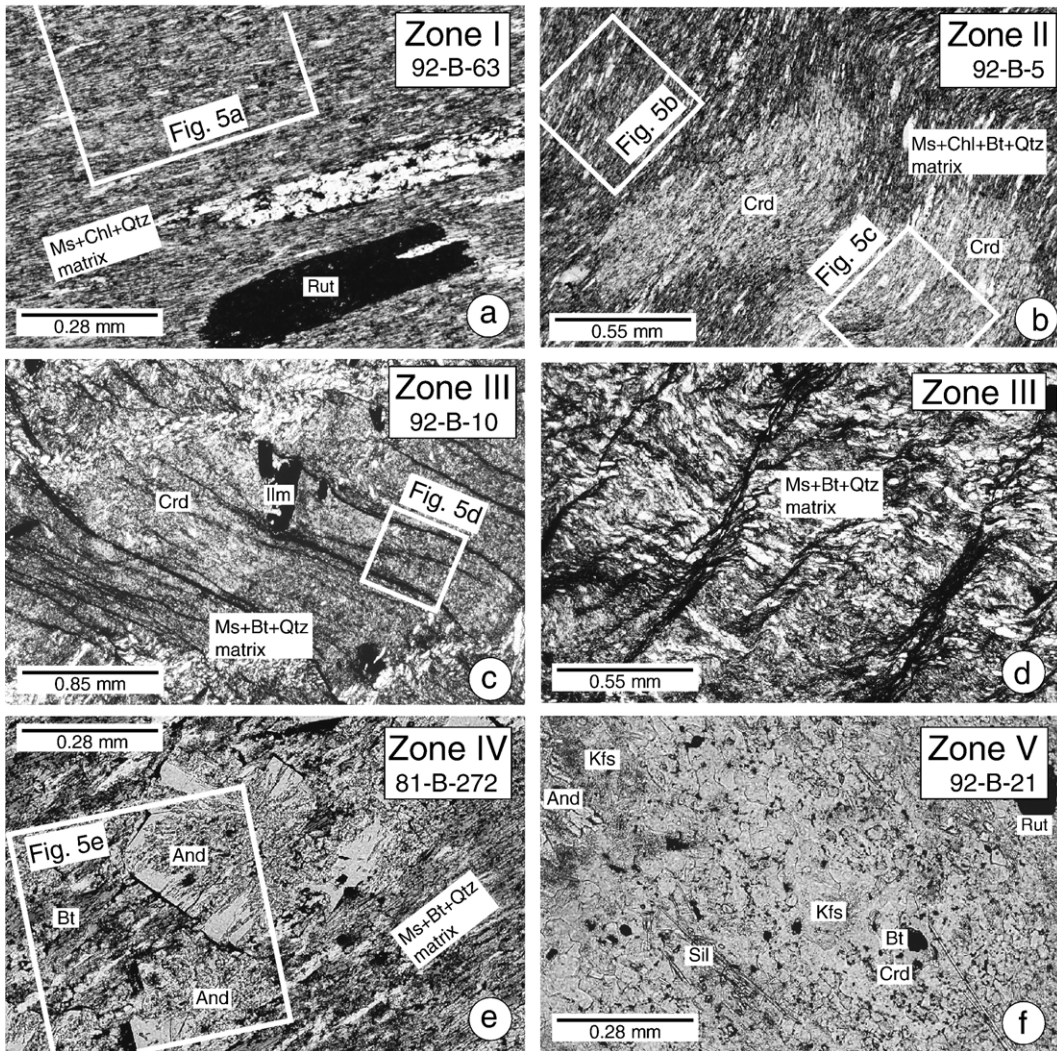


Fig. 4. Photomicrographs of graphite distribution and texture in the five zones of contact metamorphism in the Ballachulish aureole. (a) Zone I—finely dispersed graphite in slate matrix, showing the dominant regional S_2 schistosity developed prior to contact metamorphism. (b) Zone II—cordierite porphyroblasts overprinting gently folded S_2 schistosity. Graphite distribution and texture is similar in the matrix and in cordierite. (c) Zone III—cordierite porphyroblast overprinting crenulated S_2 schistosity. Graphite is concentrated in seams along the spaced crenulations. The crenulations are regional deformation features that predate contact metamorphism. (d) Zone III—crenulated graphitic hornfels. (e) Zone IV—graphite caps on the margins of andalusite porphyroblasts. (f) Zone V—dispersed graphite in the matrix of a strongly recrystallized hornfels. The larger, discrete black grains are rutile.

The finely disseminated graphite in Zone I, evident as fine black specks distributed evenly through the matrix in the optical image (Fig. 4a) is matched by a similar distribution of high-carbon specks in the carbon X-ray image (Fig. 5a). The concentration of graphite into seams along crenulation cleavages seen in the optical image in Fig. 4c is imaged as high-carbon ‘streaks’ in the carbon X-ray image in Fig. 5d. Graphite ‘caps’ on the margins of andalusite crystals in the optical image in Fig. 4e are imaged clearly in the carbon X-ray image in Fig. 5e. The

distribution of relatively coarse grained, discrete graphite grains in the rock matrix in Fig. 4f is matched in the carbon X-ray image in Fig. 5f.

Some features in the carbon X-ray maps are surface-related artifacts, recognizable by anomalous shape, size or distribution. Although the identity of these features is not always clear, possibilities include microdroplets of oil from polishing, bubbles in the carbon coat that develop during electron bombardment, flakes of carbon coat, and accumulation of carbon in pits or other surface

imperfections during polishing or coating (see caption to Fig. 5 for examples). Epoxy within cracks creates a strong high-carbon signal (Fig. 5c). Overall, however, these artifacts do not obscure the underlying patterns of graphite distribution and texture.

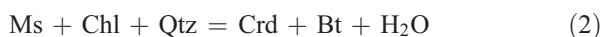
3.3. Zone I: graphitic metapelites outside of the contact aureole

Outside of the aureole, the graphitic metapelites are dark grey slates and phyllites with some silty layers (Fig. 3a). Where iron sulfides are present, pyrite is dominant >ca. 2300 m from the contact and pyrrhotite is dominant <ca. 1700 m from the contact, both occurring in the intervening interval (Neumann, 1950 and this study). Immediately downgrade of the cordierite isograd, the major phases in the rocks are quartz, muscovite, chlorite and albitic plagioclase. Accessory minerals include graphite and some or all of pyrrhotite, pyrite (rare), rutile, ilmenite (rare), phosphate phases and various detrital phases. Regional deformation prior to contact metamorphism resulted in one dominant cleavage/schistosity (S_2 in the terminology of Pattison and Voll, 1991) and local overprinting crenulations and crenulation cleavages (see further discussion under Zone III).

Graphite is generally very fine grained (<1 μm) and distributed evenly through the matrix in Zone I (Figs. 4a and 5a). The crystallographic state of the graphite was not determined, but based on the metapelites having experienced regional metamorphic temperatures of 450–500 °C, it is likely that much of the graphite is well ordered (Wang, 1989), although there is expected to be variability in individual samples (e.g. Buseck and Huang, 1985).

3.4. Zone II: cordierite + chlorite zone

Zone II is marked by the first appearance of cordierite, accompanied by biotite, and represents the first main mineralogical change in the graphitic metapelites related to contact metamorphism. The rocks develop prominent ‘spots’ (Fig. 3b), corresponding in thin section to anhedral, inclusion-rich cordierite porphyroblasts that overgrow the regional foliation (Fig. 4b). The reaction introducing Crd+Bt is:



ca. 550 °C (Pattison and Harte, 1985, 1991). Fig. 6a shows the location of this reaction in pressure–temperature space. Although reaction (2) is divariant in the chemical system K_2O – FeO – MgO – Al_2O_3 – SiO_2 – H_2O

(KFMASH), the divariant interval is predicted to be only about 2 °C wide and therefore appears as a single line in Fig. 6a. In the field, Zone II is approximately 120 m wide (Fig. 1), which corresponds to a temperature interval of 10 °C or so according to the thermal modeling of Buntebarth (1991). This minor discrepancy may reflect kinetic inhibitions to reaction progress in some of the natural rocks.

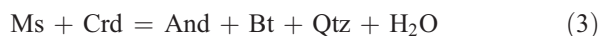
The texture and distribution of graphite in the rock matrix in Zone II (Figs. 4b and 5b) appears to be about the same as within cordierite porphyroblasts (Fig. 5c), and not significantly different from the regional grade slates and phyllites (compare Figs. 4a,b and 5a,b).

3.5. Zone III: cordierite zone

Compared to Zone II, Zone III is characterized by the absence of primary chlorite and the more prominent development of cordierite porphyroblasts (Fig. 3c), leading to the rocks having a more hornfelsic texture. Zone III is the widest metamorphic zone in the aureole. Although a range of graphite distribution and texture is seen in this zone (Figs. 4c,d and 5d), including crenulations and the development of graphitic seams, most of the features have been inherited from the regional protolith. Comparison of the carbon X-ray map in Fig. 5d with those for Zones I and II in Fig. 5a,b reveals little indication of significant textural change of graphite in Zone III.

3.6. Zone IV: andalusite + cordierite zone

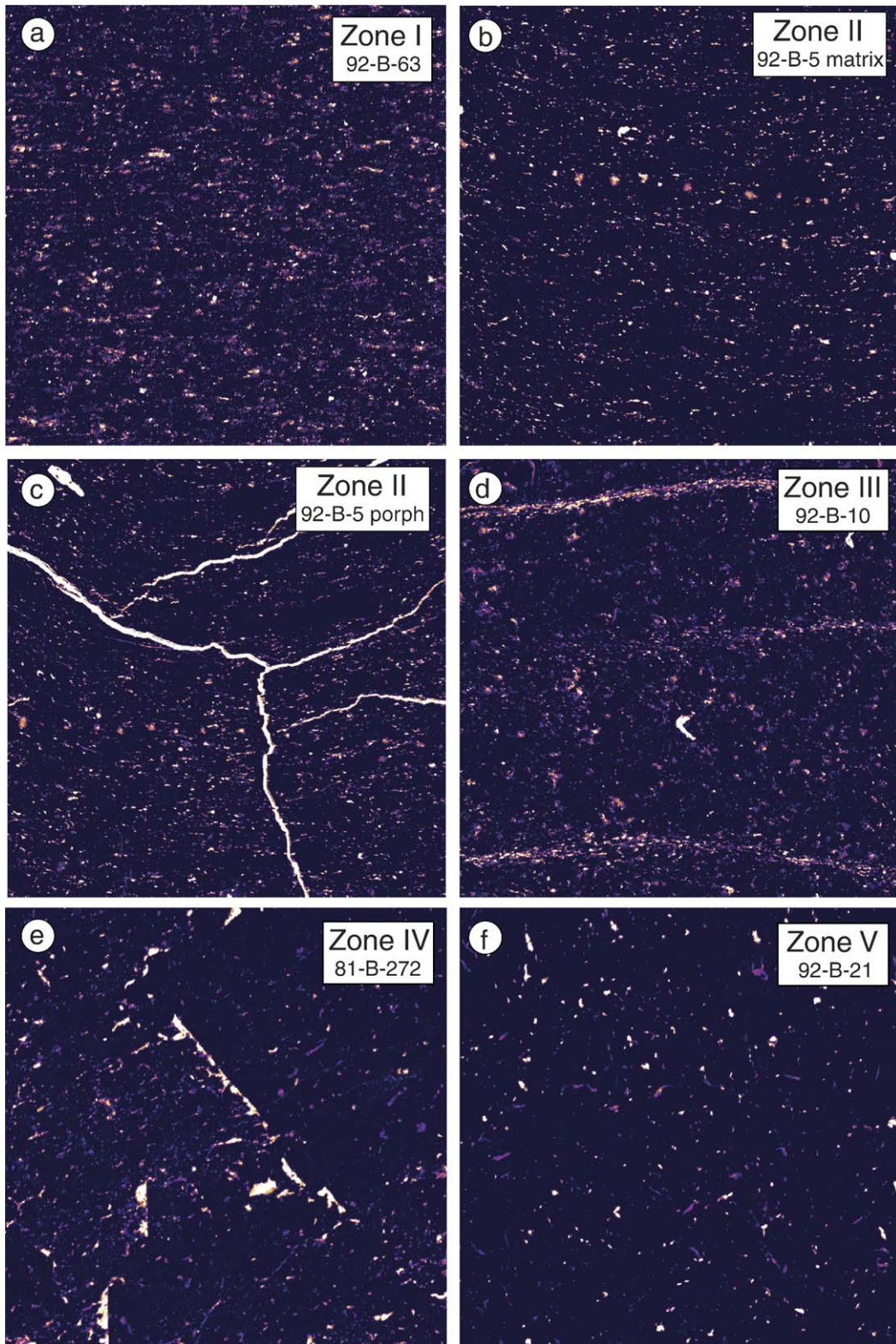
Zone IV is marked by the development of andalusite in some, but not all, rocks (Fig. 3d). The two most common assemblages in this zone are And+Crd+Bt and Crd+Bt, with the former being less common and restricted to more Fe-rich bulk compositions (Pattison et al., 2002). The Fe–Mg divariant reaction introducing andalusite to the Crd+Bt assemblage is:



ca. 600 °C (Pattison and Harte, 1985, 1991). Fig. 6a of this paper and Fig. 10 of Pattison et al. (2002) shows that this reaction has a shallow negative slope in P – T space and is strongly dependent on $\text{Mg}/(\text{Mg}+\text{Fe})$, most likely accounting for its progress in only some bulk compositions.

In contrast to cordierite, which contains graphite as minute inclusions, andalusite crystals contain relatively few graphite inclusions. Graphite commonly segre-

Carbon X-ray maps of graphitic metapelites in the Ballachulish aureole



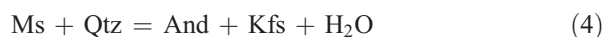
0.25 mm

gates into ‘caps’ on the margins of euhedral andalusite crystals (Figs. 4e and 5e), a consequence of the pushing aside and resultant concentration of graphite at the crystal surfaces as the andalusite grows outwards into the matrix. This is the first graphite texture that can be ascribed exclusively to contact metamorphic processes, and marks a significant modification of the texture of graphite at lower grade (compare with Fig. 5a,b and c). Graphite in the matrix of the rock, away from the andalusite crystals, appears to be somewhat more discrete and coarser grained than in Zone III (compare Fig. 5c and e).

3.7. Zone V: *andalusite* ± *sillimanite* + *K-feldspar* zone

Zone V is marked by the development of K-feldspar and the demise of primary muscovite. The rocks take on a distinctly massive, hornfelsic texture (Figs. 3e and 4f). Many of the rocks in Zone V have a light-medium brown colour in outcrop and hand sample compared to the medium-dark grey colour of the rocks at lower grade. These brown rocks have experienced severe hydrothermal alteration, revealed by abundant secondary muscovite and chlorite and completely altered cordierite, which complicates interpretation of their whole rock carbon content and texture. The most likely fluid source for the later alteration is fluid released from or focused by the subjacent intrusion (Fig. 1).

In the higher grade parts of Zone V, sillimanite appears (Fig. 4f) and locally there is evidence for partial melting (Pattison and Harte, 1988, 2001; Harte et al., 1991a). The reaction introducing K-feldspar is:



ca. 625 °C (Pattison and Harte, 1985, 1991). Fig. 6a shows the location of this reaction in *P–T* space.

Graphite in the matrix of fresh Zone V rocks (Figs. 4f and 5f) occurs in more widely spaced, coarser grains than at lower grade (compare with Figs. 4a–e and 5a–

e), and overall appears to be in lower abundance. The most severely altered rocks from Zone V appear ‘bleached’ in hand sample and thin section, with graphite scarce in the matrix but still present in altered cordierite poikiloblasts.

3.8. Summary

The whole rock carbon analysis and observational data show that graphite persists to the highest grades. Graphite abundance shows a fairly large scatter and no significant variation with grade, except for a possible decrease in the highest grade rocks (Zone V). Variable graphite abundance in rocks at the same grade reflects primary sedimentological heterogeneity, which obscures grade-related changes.

Texturally, graphite shows a tendency to form larger and more widely spaced grains in the matrix of the rocks as grade increases, consistent with expectations of grain coarsening with increasing temperature and recrystallization (e.g., Joesten, 1991). The most noticeable step in both whole rock C content and texture is between Zones IV and V, corresponding to major recrystallization accompanying the development of K-feldspar at the expense of primary muscovite. Segregation of graphite into caps on the margins of andalusite crystals is a local textural modification in some rocks from Zone IV. The overall trend of grain size increase is superimposed on more pronounced mechanically-induced features developed during regional deformation prior to contact metamorphism, such as graphite seams along crenulation cleavages.

3.9. Implications for electrical conductivity

From the perspective of electrical conductivity, the relatively coarse scale of observation of the texture and distribution of graphite compromises the ability to make firm conclusions. Enhanced electrical conductivity has been shown in a number of studies (e.g., Frost et

Fig. 5. Carbon X-ray maps showing graphite distribution and texture in the five zones of contact metamorphism in the Ballachulish aureole. Graphite appears as bright areas and spots in the image. The preferred E–W grain of the images corresponds to the dominant schistosity in the samples, formed prior to contact metamorphism. (a) Zone I—finely dispersed graphite in slate matrix (see Fig. 4a for location of image area). (b) Zone II—finely dispersed graphite in the matrix to a Ms+Chl+Crd+Bt hornfels (see Fig. 4b for location of image area). The discrete, globule-shaped domains of elevated carbon running subhorizontally across the top half of the image are most likely oil droplets on the surface of the sample, whereas the bright domain above the line of globules is an unidentified surface artifact. (c) Zone II—finely dispersed graphite within a cordierite porphyroblast in the same rock as in (b) (see Fig. 4b for location of image area). The prominent white lines are epoxy. The bright domain in the upper left of the image is an unidentified surface artifact. (d) Zone III—graphite concentrated along seams within crenulation cleavages (see Fig. 4c) and dispersed within the matrix between seams. Large, isolated bright domains are surface artifacts. (e) Zone IV—graphite caps on the margins of andalusite porphyroblasts (see Fig. 4e for location of image area). The distribution of graphite in the matrix is seen on the left side of the image. (f) Zone V—discrete graphite domains in the matrix of a strongly recrystallized hornfels (see Fig. 4f for a photomicrograph of a similar area to that imaged here).

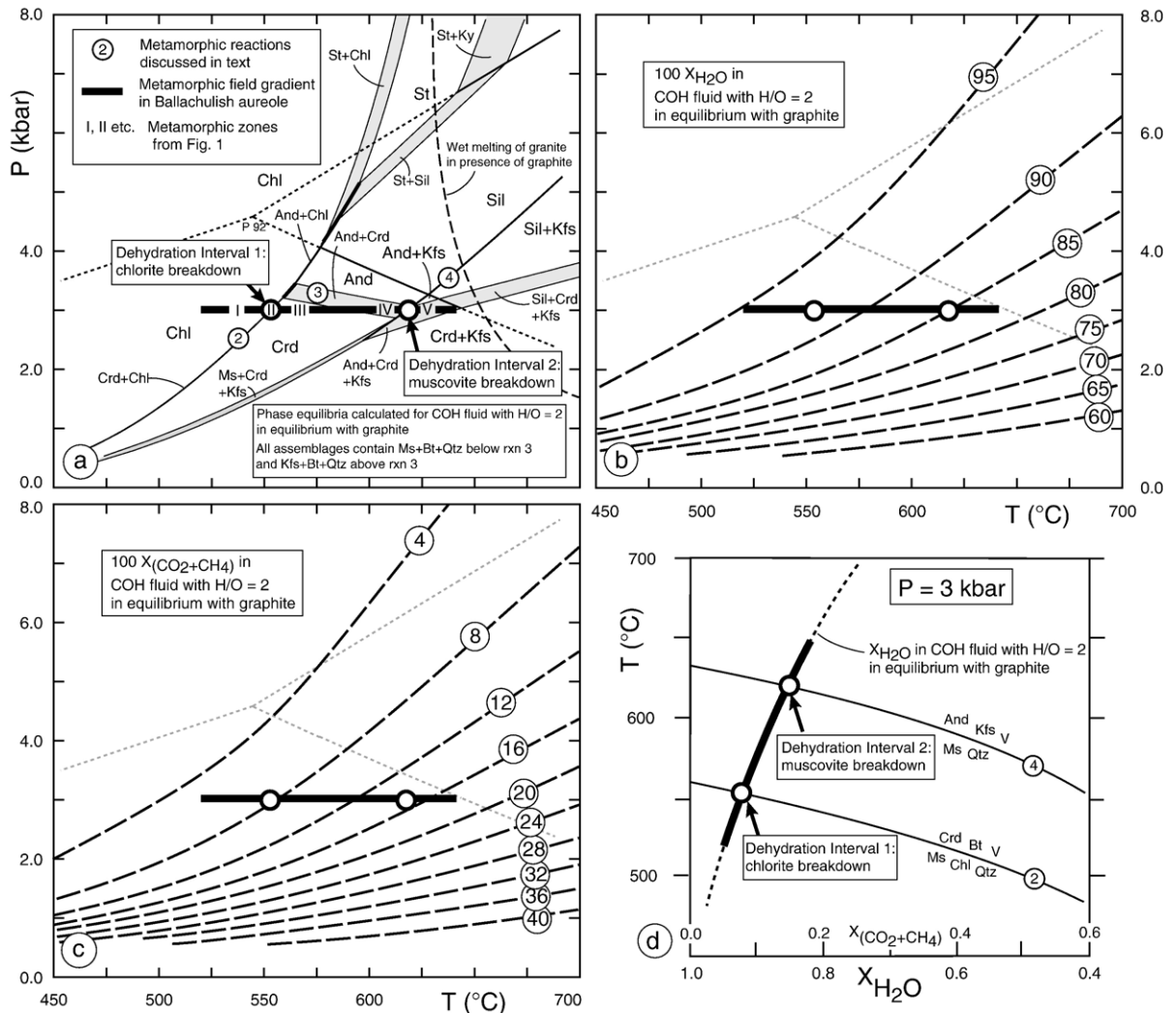


Fig. 6. (a) Pressure–temperature diagram showing mineral assemblage stability fields for average Ballachulish metapelite bulk composition, calculated for a fluid phase in equilibrium with graphite (see text for details). P_{92} - Al_2SiO_5 triple point of Pattison (1992). The wet melting curve in equilibrium with graphite comes from Cesare et al. (2003b). Reactions (2) (3) and (4) are the isograd reactions in the aureole. The metamorphic zones, metamorphic field gradient and two main dehydration intervals are discussed in the text. (b) Contours of $100 X_{H_2O}$ in a C–O–H fluid with $H/O=2$ in equilibrium with graphite, from Connolly and Cesare (1993). (c) Contours of $100 X_{CO_2+CH_4}$ in a C–O–H fluid with $H/O=2$ in equilibrium with graphite, from Connolly and Cesare (1993). (d) Isobaric temperature– X_{H_2O} diagram, calculated at the 3 kbar pressure of contact metamorphism at Ballachulish, showing the temperature-dependence of reactions (2) and (4) on X_{H_2O} , and the T – X_{H_2O} path of graphitic metapelites going upgrade in the aureole. Corresponding values of $X_{CO_2+CH_4}$ are also shown.

al., 1989; Shankland et al., 1997; Mogk and Mathez, 2000; Crespo et al., 2004) to depend on thin nanometer-scale graphite films that cannot be imaged using the electron microprobe. Considering only the micron-scale changes documented in this study, the effects of prograde contact metamorphism are expected to result in broadly diminished conductivity, due to the development of more widely spaced, discrete graphite flakes insulated by non-conducting silicate minerals at high grade compared to low grade (compare Fig. 5a,f). These thermally induced prograde metamorphic effects

are likely of secondary importance compared to the effects of mechanically induced graphite segregation (cf. Jödicke et al., 2004).

4. Thermodynamic calculations of graphite consumption during prograde contact metamorphism

A quantitative estimate of graphite consumption during contact metamorphism at Ballachulish is attempted to compare with the findings from whole rock C analysis.

The approach involves calculating the amount of graphite that dissolves into, and is carried away by, the metamorphic fluid phase under the following assumptions: only outward fluid movement (no fluid infiltration into the rocks); no re-deposition of graphite from cooled C–O–H fluids in the pores of the rocks; and internally controlled fO_2 (more details below).

Two main dehydration intervals occur in the aureole: (1) the consumption of chlorite by reaction (2) to produce cordierite; and (2) the consumption of muscovite by reaction (4) to produce andalusite and K-feldspar. Production of andalusite in Zone IV by reaction (3) has been ignored in the treatment that follows because this assemblage is only locally developed, reaction progress is expected to be minor due to the shallow P – T slope of the reaction, and the reaction itself produces only a small amount of water, arising from the release of structurally bound water in cordierite (Pattison et al., 2002).

The numbered mineral reactions, metamorphic field gradient at Ballachulish, and the two main dehydration reactions are shown in the P – T diagram in Fig. 6a. Fig. 6a was calculated for an average Ballachulish pelite bulk composition in the chemical system K_2O – FeO – MgO – Al_2O_3 – SiO_2 – H_2O (KFMASH) assuming a fluid phase in equilibrium with graphite (see below). In terms of the Thompson (1957) AFM projection, the bulk composition has an A value of 0.1 and $Mg/(Mg+Fe)$ of 0.46. The calculations were made using: the Gibbs software of Spear (1988, 1990) and Spear et al. (2001); the thermodynamic data set of Spear, Pattison and Cheney, reported in Pattison et al. (2002); and the thermodynamic expressions for C–O–H fluids of Connolly and Cesare (1993). Further details on the calculation of the same type of diagram are found in Pattison and Vogl (2005).

4.1. C–O–H fluids in equilibrium with graphite

Equilibration of graphite with water is represented by the reaction:



Connolly and Cesare (1993) argued that C–O–H fluids produced by the equilibration of graphite with water generated from dehydration reactions must maintain the H/O atomic ratio of water, 2:1, thereby uniquely determining all the thermodynamic properties of the fluid at a given P – T condition, including oxygen fugacity. This constraint is illustrated in the C–O–H ternary diagram and fO_2 – $\log X_i$ diagram in

Fig. 7a,b. At P – T conditions of normal crustal metamorphism, the resultant C–O–H fluid is essentially an H_2O –dominated H_2O – CO_2 – CH_4 mixture, with other species making up less than 1% of the fluid. The fluid has a maximum X_{H_2O} and sensibly equal concentrations of CO_2 and CH_4 (Connolly and Cesare, 1993; see Fig. 7b). As temperature increases, the fO_2 of the H/O=2 fluid in equilibrium with graphite cuts across iron oxide and silicate fO_2 buffers towards relatively more reducing conditions (Fig. 7c).

In some rocks, the presence of pyrrhotite implies the presence of S species in the fluid, mainly H_2S . Although H_2S reduces X_{H_2O} in the fluid phase and alters the balance of carbon-bearing fluid species, it has a modest effect on total dissolved carbon (compare Figs. 1c and 5c of Connolly and Cesare, 1993). For this reason, the effects of sulfur have been ignored.

Fig. 6b,c show the variation in P – T space of X_{H_2O} and X_{CO_2} , respectively, in a C–O–H fluid with H/O=2 in equilibrium with graphite. Fig. 6d shows the evolution of the fluid in a T – X_{H_2O} diagram at a fixed pressure of 3 kbar, the estimated pressure of contact metamorphism at Ballachulish. These diagrams show that the carbon content of the fluid increases with increasing temperature, but is still dominated by H_2O . The C–O–H fluid at conditions of chlorite breakdown (ca. 550 °C) contains 92% H_2O and 4% each of CO_2 and CH_4 , whereas at conditions of muscovite breakdown (ca. 625 °C) it contains 85% H_2O and 7.5% each of CO_2 and CH_4 (Fig. 6b,c).

4.2. Graphite consumption during contact metamorphism

A model rock composition, representative of average Ballachulish graphitic metapelite outside of the aureole, was used to predict how much graphite would be consumed during contact metamorphism. The model modal mineralogy is 20% chlorite, 30% muscovite, 35% quartz, 14% plagioclase and accessory phases, and 1% graphite (Chl:Ms:Qtz:Pl:Gr=20:30:35:14:1). Plagioclase and accessory phases are assumed to be uninvolved in the reactions. Assuming 1000 cm³ of rock, and average mineral compositions at Ballachulish (Pattison, 1987), this results in a rock with 5.9 moles of H_2O tied up in chlorite and muscovite. All reaction was assumed to occur at the two main dehydration intervals involving chlorite and muscovite breakdown (reactions 2

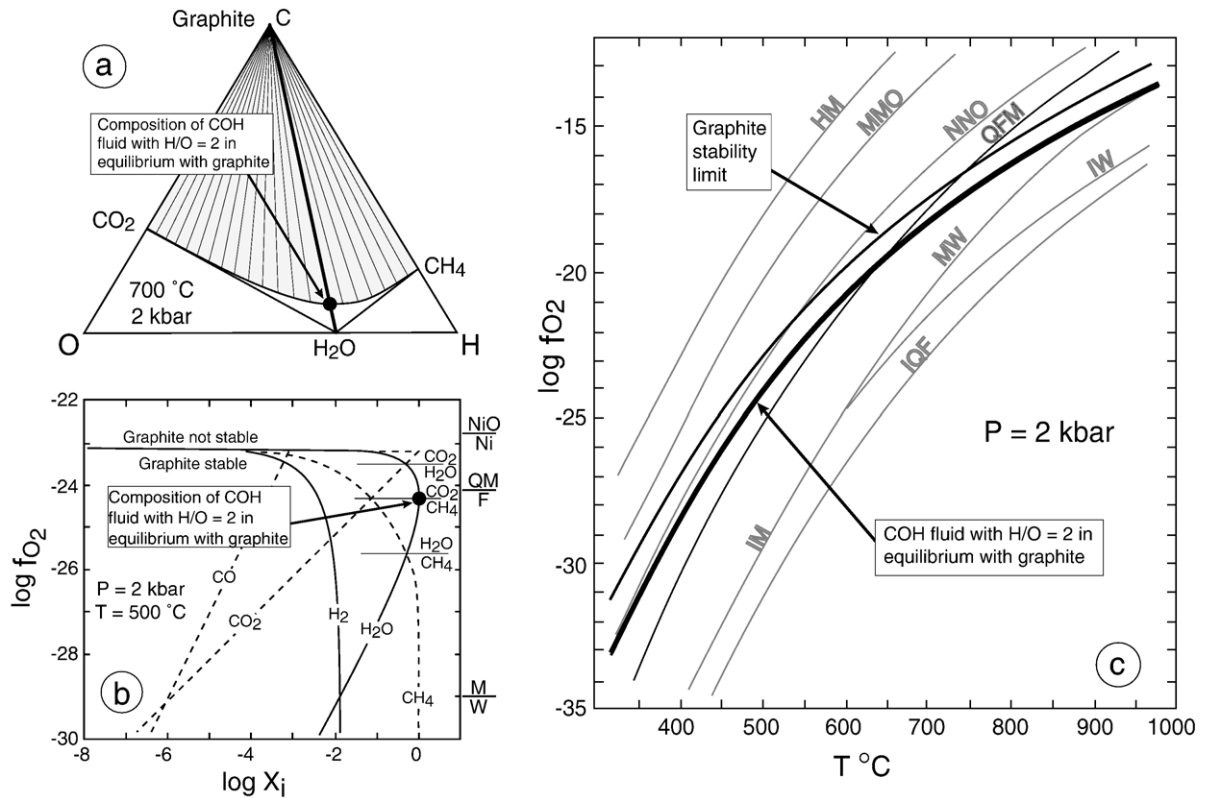


Fig. 7. (a) Isobaric, isothermal C–O–H diagram showing the graphite–fluid surface and the unique fluid composition that results from assuming an H:O ratio of 2:1. Modified from Fig. 18–13e of Spear (1993), based on Ferry and Baumgartner (1987). (b) Isobaric, isothermal log f_{O_2} –log X_i diagram, showing concentrations of C–O–H fluid species as a function of f_{O_2} . The solid dot shows the composition of an H/O=2 fluid in equilibrium with graphite, corresponding to a condition of maximum X_{H_2O} . Modified from Fig. 18–8 of Spear (1993), based on Ohmoto and Kerrick (1977). (c) Isobaric log f_{O_2} –temperature diagram, illustrating how a C–O–H fluid with H/O=2 in equilibrium with graphite is an f_{O_2} buffer that cuts across common oxide and silicate oxygen buffers to relatively more reducing conditions. HM–Fe₂O₃–Fe₃O₄. MMO–Mn₃O₄–MnO. NNO–Ni–NiO. QFM–SiO₂–Fe₂SiO₄–Fe₃O₄. MW–Fe₃O₄–FeO. IM–Fe–Fe₃O₄. IW–Fe–FeO. IQF–Fe–SiO₂–Fe₂SiO₄. Modified from Fig. 18–9b of Spear (1993), based on Ohmoto and Kerrick (1977).

and 4). The stoichiometry for the two reactions (Pattison, 1989), assuming cordierite with 0.5 moles of structurally bound water, is:



Cordierite is assumed to maintain 0.5 mol of water going upgrade, a simplification with negligible consequences for the calculations. Carbon was removed from the rock at these two dehydration intervals assuming it dissolved into the fluid in the proportions shown in Fig. 6b and c and listed above.

The results are shown in Table 1 and Fig. 8. In Fig. 8, the width of the two reaction intervals is exaggerated, compared to that seen in the field, to show more clearly the modal changes across the reactions. Of the 5.9 mol of water in the protolith,

56% is lost with the consumption of chlorite, and a further 20% is lost with the consumption of muscovite. The remaining 24% is retained in biotite and

Table 1
Calculated modal variations at Ballachulish

	Zone		
	I	III	V
Graphite	1.00	0.87	0.77
Chlorite	20.0	0.0	0.0
Muscovite	30.0	16.8	0.0
Quartz	35.0	31.2	28.6
Plagioclase	14.0	14.2	14.2
Cordierite	0.0	22.5	22.6
Biotite	0.0	14.6	14.6
Andalusite	0.0	0.0	6.2
K-feldspar	0.0	0.0	13.0
Total	100.0	100.0	100.0
Moles H ₂ O/ 1000 cc rock	5.9	2.6	1.4
% of H ₂ O in original rock	100	44	24

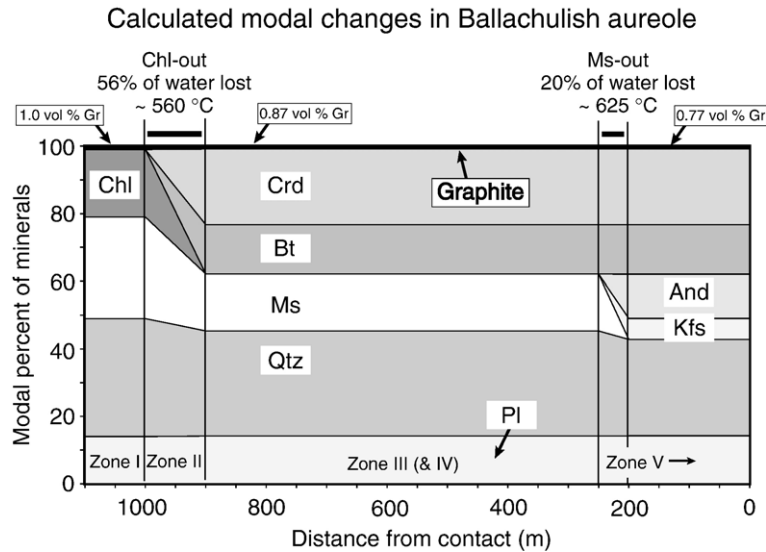


Fig. 8. Calculated modal changes in model Ballachulish metapelite going up grade along the isobaric P – T path shown in Fig. 6a (see text for details).

cordierite. Graphite decreases from 1.0 vol.% in the protolith to 0.87 vol.% following consumption of chlorite to 0.77 vol.% following consumption of muscovite, a net decrease of 0.23 vol.%. This volume is equivalent to 0.19 wt.% carbon.

Different proportions of chlorite and muscovite result in different amounts of graphite consumption. For a semipelitic protolith with Chl:Ms:Qtz:Pl:Gr=5:10:50:34:1, the predicted graphite consumption is 0.07 vol.%, whereas for a muscovite-rich pelitic rock with Chl:Ms:Qtz:Pl:Gr=10:50:29:10:1, the predicted graphite consumption is 0.32 vol.%, with most of the graphite being consumed during muscovite breakdown (0.26 vol.%). The expected range of graphite consumption for reasonable metapelite starting compositions is therefore 0.1–0.3 vol.%. Metapelites with more than this amount of graphite will retain graphite throughout prograde contact metamorphism.

An additional unquantified factor is the effect of retrograde alteration due to post-peak fluid infiltration, such as in Zone V. This process will cause further graphite dissolution, the amount of which depends on the amount of fluid infiltration and the temperature at which infiltration occurred. Given the evidence for relatively low temperature hydrothermal alteration, such as the replacement of cordierite by chlorite and muscovite, substantial fluid infiltration would be required to dissolve a significant amount of graphite because of its low solubility in low temperature fluids (Fig. 6b and c).

4.3. Comparison with whole rock analysis and textural features

The predicted amount of graphite consumed due to contact metamorphism (0.1–0.3 vol.%) is less than the average measured amount of graphite in the metapelites outside the aureole (ca. 0.8 vol.%, based on an average whole rock C content of 0.67 wt.%). Most graphitic metapelites are therefore predicted to retain graphite through contact metamorphism, consistent with the whole rock and observational data. Adding the amount of carbon predicted to be consumed during contact metamorphism to the present carbon content of the two highest grade, Zone V rocks (ca. 0.35 wt.%, equivalent to 0.42 vol.% graphite) results in a carbon content similar to the rocks outside of the aureole.

The predicted amount of graphite consumed due to contact metamorphism is less than the natural variation in graphite abundance in individual metamorphic zones, accounting for the scatter in whole rock C content and lack of a strong trend as a function of metamorphic grade (see Fig. 2). Whereas there appears to be a significant drop in carbon content between Zones IV and V, consistent with graphite consumption due to muscovite dehydration, there is no evidence for a drop between Zones I and III in which chlorite is consumed, even though over half of the graphite is predicted to be consumed at this step (Table 1 and Fig. 8). Either the primary heterogeneity of the rocks masks this drop, or the model protolith in

Table 1 and Fig. 8 contains too much chlorite, resulting in an overestimate of the amount of graphite predicted to be consumed at the chlorite-out reaction. The muscovite-rich protolith modeled above, in which ca. 0.3 vol.% graphite is consumed at the muscovite-out isograd, results in a predicted trend of graphite consumption that more closely matches the measured trend, but may not be representative of the majority of the graphitic metapelites. Finally, the marked alteration in Zone V may contribute to the drop-off in C abundance in that zone.

5. Implications for regional prograde metamorphism of metapelites

Examination of Fig. 6 shows that the solubility of carbon in C–O–H fluid, and therefore the amount of graphite that is consumed during prograde metamorphism, decreases as pressure increases. Consequently, the results of this study of relatively low pressure contact metamorphism provide a maximum estimate of expected graphite consumption during regional metamorphism. For regional Barrovian metamorphism that reaches mid- to upper-amphibolite facies conditions (stability of Kfs+Sil), chlorite-bearing metapelitic rocks containing as little as 0.1–0.2 vol.% graphite are expected to retain graphite through prograde metamorphism.

Connolly and Cesare (1993) noted that in graphitic rocks undergoing dehydration, graphite-water will be the dominant f_{O_2} buffer in the rock, overwhelming the effects of oxidation of Fe^{3+} in coexisting oxides and silicates and all but the most extreme scenarios of fluid infiltration. The effectiveness of graphite as an oxygen buffer is shown in their Fig. 1d, which shows the volumetric ratio of graphite to fluid as a function of P and T . This ratio exceeds 100 for regional metamorphic conditions, which translates to only 0.1 vol.% graphite being required to saturate a C–O–H fluid in a rock that generates 4 wt.% H_2O (ca. 6.1 mol H_2O per 1000 cm^3 of rock), similar to the results of this study. Thus, even for metapelites containing a small amount of graphite, f_{O_2} will be buffered throughout metamorphism.

Acknowledgements

I thank Rob Marr for the help with the carbon mapping, Andy Tomkins for comments on the first draft of the paper, and Bernard Cesare and Ed Mathez for their helpful reviews. This research was supported by NSERC Research Grant 0037233.

References

- Beysac, O., Goffé, B., Chopin, C., Rouzaud, J.N., 2002. Raman spectra of carbonaceous material in metasediments: a new geothermometer. *Journal of Metamorphic Geology* 20, 859–871.
- Buntebarth, G., 1991. Thermal models of cooling. In: Voll, G., Töpel, J., Pattison, D.R.M., Seifert, F. (Eds.), *Equilibrium and Kinetics in Contact Metamorphism: The Ballachulish Igneous Complex and its Thermal Aureole*. Springer Verlag, Heidelberg, pp. 379–404.
- Buseck, P.R., Huang, B., 1985. Conversion of carbonaceous material to graphite during metamorphism. *Geochimica et Cosmochimica Acta* 49, 2003–2016.
- Cesare, B., Meli, S., Nodari, L., Russo, U., 2003a. Fe^{3+} reduction during biotite melting in graphitic metapelites: another origin of CO_2 in granulites. *Contributions to Mineralogy and Petrology* 149, 129–140.
- Cesare, B., Marchesi, C., Hermann, J., Gomez-Pugnaire, M.T., 2003b. Primary melt inclusions in andalusite from anatectic graphitic metapelites: implications for the position of the Al_2SiO_5 triple point. *Geology* 31, 573–576.
- Connolly, J.A.D., Cesare, B., 1993. C–O–H–S fluid compositions and oxygen fugacity in graphitic metapelites. *Journal of Metamorphic Geology* 11, 379–388.
- Crespo, E., Luque, J., Fernandez, R.C., Rodas, M., Diaz, A.M., Fernandez, C.J.C., Barrenechea, J.F., 2004. Significance of graphite occurrences in the Aracena metamorphic belt, Iberian Massif. *Geological Magazine* 141, 687–697.
- Ferraris, C., Groberty, B., Green, F.G.L., Wessicken, R., 2004. Inter-growth of graphite within phlogopite from Finero ultramafic complex, Italian Western Alps; implications for mantle crystallization of primary-texture mica. *European Journal of Mineralogy* 6, 899–908.
- Ferry, J.M., 1996. Prograde and retrograde fluid flow during contact metamorphism of siliceous carbonate rocks from the Ballachulish aureole, Scotland. *Contributions to Mineralogy and Petrology* 124, 235–254.
- Ferry, J.M., Baumgartner, L., 1987. Thermodynamic models of molecular fluids at the elevated pressures and temperatures of crustal metamorphism. In: Carmichael, I.S.E., Eugster, H.P. (Eds.), *Thermodynamic Modeling of Geological Materials: Minerals, Fluids and Melts*. Mineralogical Society of America Reviews in Mineralogy, vol. 17, pp. 323–365.
- French, B.M., 1964. Graphitization of organic material in a progressively metamorphosed Precambrian iron formation. *Science* 146, 917–918.
- Fraser, G.L., Pattison, D.R.M., Heaman, L.M., 2004. Age of the Ballachulish and Glencoe Igneous Complexes (Scottish Highlands), and paragenesis of zircon, monazite and baddeleyite in the Ballachulish Aureole. *Journal of the Geological Society of London* 161, 447–462.
- Frost, B.R., Fyfe, W.S., Tazaki, K., Chan, T., 1989. Grain-boundary graphite in rocks and implications for high electrical conductivity in the lower crust. *Nature* 340, 134–136.
- Grew, E.S., 1974. Carbonaceous material in some metamorphic rocks of New England and other areas. *Journal of Geology* 82, 5–73.
- Harte, B., Pattison, D.R.M., Linklater, C.M., 1991a. Field relations and petrography of partially melted pelitic and semi-pelitic rocks. In: Voll, G., Töpel, J., Pattison, D.R.M., Seifert, F. (Eds.), *Equilibrium and Kinetics in Contact Metamorphism: the Ballachulish Igneous Complex and its Thermal Aureole*. Springer Verlag, Heidelberg, pp. 181–210.

- Harte, B., Pattison, D.R.M., Heuss-Assbichler, S., Hoernes, S., Masch, L., Strong, D.F., 1991b. Evidence of fluid phase behaviour and controls in the intrusive complex and its aureole. In: Voll, G., Töpel, J., Pattison, D.R.M., Seifert, F. (Eds.), *Equilibrium and Kinetics in Contact Metamorphism: The Ballachulish Igneous Complex and its Thermal Aureole*. Springer Verlag, Heidelberg, pp. 405–422.
- Itaya, T., 1981. Carbonaceous material in pelitic schists of the Sanbagawa metamorphic belt in central Shikoku, Japan. *Lithos* 14, 215–224.
- Jödicke, H., Kruhl, J.H., Ballhaus, C., Giese, P., Untiedt, J., 2004. Syngenetic, thin graphite-rich horizons in lower crustal rocks from the Serre San Bruno, Calabria (Italy), and implications for the nature of high-conducting deep crustal layers. *Physics of the Earth and Planetary Interiors* 141, 37–58.
- Joesten, R.L., 1991. Kinetics of coarsening and diffusion-controlled mineral growth. In: Kerrick, D.M. (Ed.), *Contact Metamorphism*, Society of America Reviews in Mineralogy, vol. 26, pp. 507–582.
- Kretz, R., 1983. Symbols for rock-forming minerals. *American Mineralogist* 68, 277–279.
- Landis, C.A., 1971. Graphitization of dispersed carbonaceous material in metamorphic rocks. *Contributions to Mineralogy and Petrology* 30, 34–45.
- Mogk, D., Mathez, E., 2000. Carbonaceous films in midcrustal rocks from the KTB borehole, Germany, as characterized by time-of-flight secondary ion mass spectrometry. *Geochemistry Geophysics Geosystems* 1 (11). doi:10.1029/2000GC000081.
- Morikiyo, T., 1986. Hydrogen and carbon isotope studies on the graphite-bearing metapelites in the northern Kiso district of central Japan. *Contributions to Mineralogy and Petrology* 94, 165–177.
- Neumann, H., 1950. Pseudomorphs of pyrrhotine after pyrite in the Ballachulish slates. *Mineralogical Magazine* 29, 234–238.
- Ohmoto, H., Kerrick, D., 1977. Devolatilization equilibria in graphitic systems. *American Journal of Science* 277, 1031–1044.
- Okuyama-Kusunose, Y., Itaya, T., 1987. Metamorphism of carbonaceous material in the Tono contact aureole, Kitagami Mountains, Japan. *Journal of Metamorphic Geology* 5, 121–139.
- Pattison, D.R.M., 1987. Variations in Mg/(Mg+Fe), F, and (Fe,Mg)-Si=2Al in pelitic minerals in the Ballachulish thermal aureole, Scotland. *American Mineralogist* 72, 255–272.
- Pattison, D.R.M., 1989. *P-T* conditions and the influence of graphite on pelitic phase relations in the Ballachulish aureole, Scotland. *Journal of Petrology* 30, 1219–1244.
- Pattison, D.R.M., 1992. Stability of andalusite and sillimanite and the Al₂SiO₅ triple point: constraints from the Ballachulish aureole, Scotland. *Journal of Geology* 100, 423–446.
- Pattison, D., Harte, B., 1985. A petrogenetic grid for pelites in the Ballachulish aureole and other Scottish thermal aureoles. *Journal of the Geological Society of London* 142, 7–28.
- Pattison, D.R.M., Harte, B., 1988. Evolution of structurally contrasting anatectic migmatites in the 3-kbar Ballachulish aureole, Scotland. *Journal of Metamorphic Geology* 6, 475–494.
- Pattison, D.R.M., Harte, B., 1991. Petrography and mineral chemistry of pelites. In: Voll, G., Töpel, J., Pattison, D.R.M., Seifert, F. (Eds.), *Equilibrium and Kinetics in Contact Metamorphism: The Ballachulish Igneous Complex and its Thermal Aureole*. Springer Verlag, Heidelberg, pp. 135–180.
- Pattison, D.R.M., Harte, B., 1997. The geology and evolution of the Ballachulish igneous Complex and Aureole. *Scottish Journal of Geology* 33, 1–29.
- Pattison, D.R.M., Harte, B., 2001. The Ballachulish Igneous Complex and Aureole: A field guide. Edinburgh Geological Society, Edinburgh, Scotland. (148 pp.)
- Pattison, D.R.M., Vogl, J.J., 2005. Contrasting sequences of metapelitic mineral-assemblages in the aureole of the tilted Nelson Batholith, British Columbia: implications for phase equilibria and pressure determination in andalusite–sillimanite type settings. *Canadian Mineralogist* 43, 51–88.
- Pattison, D.R.M., Voll, G., 1991. Regional geology of the Ballachulish area. In: Voll, G., Töpel, J., Pattison, D.R.M., Seifert, F. (Eds.), *Equilibrium and Kinetics in Contact Metamorphism: the Ballachulish Igneous Complex and its Thermal Aureole*. Springer Verlag, Heidelberg, pp. 19–38.
- Pattison, D.R.M., Spear, F.S., BeBuhr, C.L., Cheney, J.T., Guidotti, C.V., 2002. Thermodynamic modelling of the reaction Muscovite+Cordierite=Al₂SiO₅+Biotite+Quartz+H₂O: constraints from natural assemblages and implications for the metapelitic petrogenetic grid. *Journal of Metamorphic Geology* 20, 99–118.
- Shankland, T.J., Duba, A.G., Mathez, E.A., Peach, C.L., 1997. Increase of electrical conductivity with pressure as an indicator of conduction through a solid phase in midcrustal rocks. *Journal of Geophysical Research* 102, 14741–14750.
- Sobolev, N.V., Shatsky, V.S., 1990. Diamond inclusions in garnets from metamorphic rocks: a new environment for diamond formation. *Nature* 343, 742–746.
- Spear, F.S., 1988. The Gibbs method and Duhem's theorem: the quantitative relationships among *P*, *T*, chemical potential, phase composition and reaction progress in igneous and metamorphic systems. *Contributions to Mineralogy and Petrology* 99, 249–256.
- Spear, F.S., 1990. Petrologic determination of metamorphic pressure–temperature–time paths. In: Spear, F.S., Peacock, S.M. (Eds.), *Metamorphic Pressure–Temperature–Time paths*, 28th International Geological Conference — Short Course in Geology, vol. 7, pp. 1–55 (Washington, D.C.)
- Spear, F.S., 1993. *Metamorphic Phase Equilibria and Pressure–Temperature–Time Paths*. Mineralogical Society of America Monograph, vol. 1. (799 pp.)
- Spear, F.S., Pyle, J.M., Storm, L.C., 2001. Thermodynamic modelling of mineral reactions: an introduction to program Gibbs. *Northeastern Geological Society of America Short Course* 504 (on CD).
- Thompson, J.B., 1957. The graphical analysis of mineral assemblages in pelitic schists. *American Mineralogist* 42, 842–858.
- Voll, G., Töpel, J., Pattison, D.R.M., Seifert, F. (Eds.), *Equilibrium and Kinetics in Contact Metamorphism: the Ballachulish Igneous Complex and its Aureole*. Springer Verlag, Heidelberg. (484 pp.)
- Wang, G., 1989. Carbonaceous material in the Ryoke metamorphic rocks, Kinki district, Japan. *Lithos* 22, 305–316.
- Weiss, S., Troll, G., 1989. The Ballachulish Igneous Complex, Scotland: Petrography, mineral chemistry and order of crystallisation in the monzodiorite–quartz diorite suite and in the granite. *Journal of Petrology* 30, 1069–1116.
- Weiss, S., Troll, G., 1991. Thermal conditions and crystallisation sequence in the Ballachulish Complex. In: Voll, G., Töpel, J., Pattison, D.R.M., Seifert, F. (Eds.), *Equilibrium and Kinetics in Contact Metamorphism: The Ballachulish Igneous Complex and its Thermal Aureole*. Springer Verlag, Heidelberg, pp. 67–98.
- Wopenka, B., Pasteris, J.D., 1993. Structural characterization of kero-gens to granulite-facies graphite— applicability of Raman micro-probe spectroscopy. *American Mineralogist* 78, 533–557.